

SPIN-SHAPE MODEL FOR 374 BURGUNDIA

Lorenzo Franco
Balzaretto Observatory (A81), Rome, ITALY
lor_franco@libero.it

Alessandro Marchini, Riccardo Papini
Astronomical Observatory, DSFTA - University of Siena (K54)
Via Roma 56, 53100 - Siena, ITALY

Giorgio Baj
M57 Observatory (K38), Saltrio, ITALY

Giulio Scarfi
Iota Scorpii Observatory (K78), La Spezia, ITALY

Fabio Mortari
Hypatia Observatory (L62), Rimini, ITALY

Pietro Aceti
Seveso Observatory (C24), Seveso, ITALY

Richard E. Schmidt
Burlleith Observatory (I13), Washington, DC 20007 USA

Robert A. Koff
Antelope Hills Observatory (H09), Bennett, CO 80102 USA

(Received: 2021 April 10. Revised: 2021 May 22)

We present a shape and spin axis model for main-belt asteroid 374 Burgundia. The model was achieved with the lightcurve inversion process, using combined dense photometric data acquired from four apparitions between 2000-2021 and sparse data from USNO Flagstaff. Analysis of the resulting data found a sidereal period $P = 6.96397 \pm 0.00002$ hours and two mirrored pole solutions at $(\lambda = 9^\circ, \beta = 38^\circ)$ and $(\lambda = 178^\circ, \beta = 28^\circ)$ with an uncertainty of ± 10 degrees.

The Minor planet 374 Burgundia was recently observed by the Italian Amateur Astronomers Union (UAI; 2021) group in order to acquire data for lightcurve inversion work (Franco et al. 2019, 2021). Other dense photometric data were downloaded from ALCDEF (ALCDEF, 2021) and, to improve the coverage at various aspect angles, was used sparse data from USNO Flagstaff Station, downloaded from the Asteroids Dynamic Site (AstDyS-2, 2020), according Durech et al. (2009).

The observational details of the dense data used are reported in Table I with the mid-date, number of the lightcurves used for the inversion process, longitude and latitude of phase angle bisector ($LPAB$, $BPAB$).

Reference	Mid-date	# LC	$LPAB^\circ$	$BPAB^\circ$
Koff (2000) (*)	2000-11-15	3	41	-1
Schmidt (2017) (*)	2017-07-10	9	245	6
Franco et al. (2019)	2018-09-27	7	354	8
Franco et al. (2021)	2021-03-04	8	169	-9

Table I. Observational details for the data used in the lightcurve inversion process for 374 Burgundia.
(*) Published on 'alcdef.org' web site.

Lightcurve inversion was performed using *MPO LCInvert* v.11.8.2.0 (BDW Publishing, 2016). For a description of the modeling process see LCInvert Operating Instructions Manual, Durech et al. (2010); and references therein.

Figure 1 shows the PAB longitude/latitude distribution for the dense and sparse data used in the lightcurve inversion process. Figure 2 (top panel) shows the sparse photometric data distribution (intensities vs JD) and (bottom panel) the corresponding phase curve (reduced magnitudes vs phase angle).

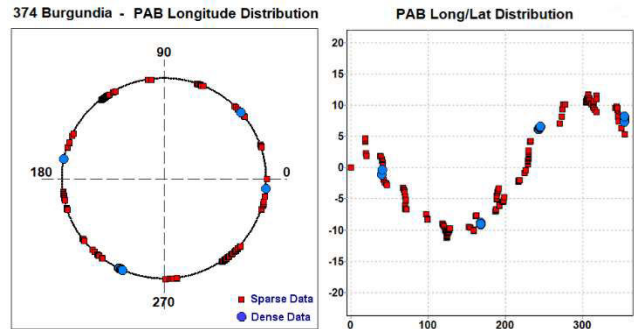


Figure 1: PAB longitude and latitude distribution of the data used for the lightcurve inversion model.

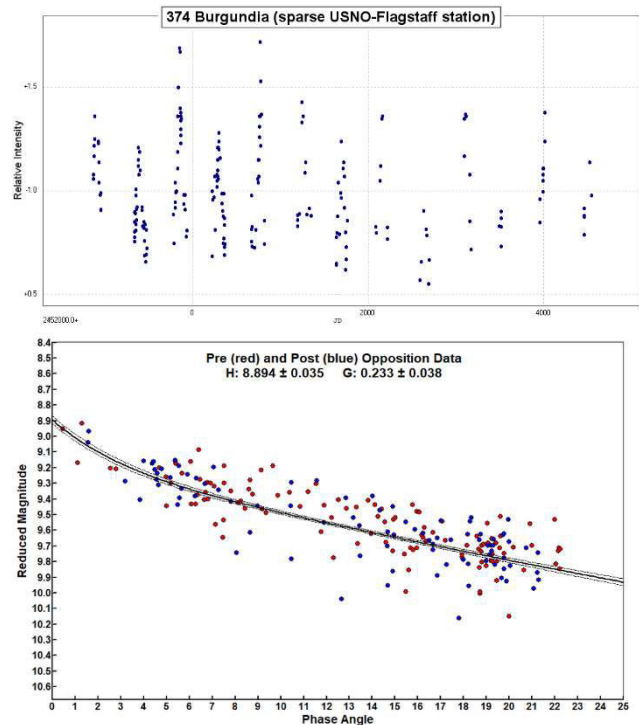


Figure 2: Top: sparse photometric data point distribution from (689) USNO Flagstaff station (relative intensity of the asteroid's brightness vs Julian Day). Bottom: phase curve obtained from sparse data (reduced magnitude vs phase angle).

In the analysis the processing weighting factor was set to 1.0 for dense data and 0.3 for sparse data. The “dark facet” weighting factor was set to 0.7 to keep the dark facet area below 1% of total area and the number of iterations was set to 50.

In lightcurve inversion work the critical step is to find an accurate sidereal rotational period. For this purpose, we started the period scan around about the 3-sigma interval centered on the average of the synodic periods found in the asteroid lightcurve database (LCDB; Warner et al., 2009). We found one isolated sidereal period with a Chi-Sq value within 10% of the lowest Chi-Sq (Figure 3), according to the criterion for the “unique solution” defined by Durech et al. (2009).

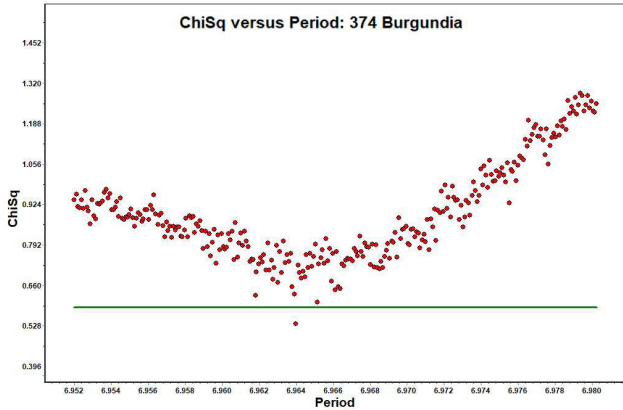


Figure 3: The period scan for 374 Burgundia shows one isolated sidereal period with Chi-Sq values within 10% of the lowest value.

The pole search was started using the “medium” search option (312 fixed pole position with 15° longitude-latitude steps) and the previously found sidereal period set to “float”. From this step we found two roughly mirrored lower Chi-Sq solutions (Figure 4) separated by about 180° in longitude at ecliptic longitude-latitude pairs (15°, 45°) and (180°, 30°).

The subsequent “fine” search option (49 fixed pole steps with 10° longitude-latitude pairs set to “float”) allowed us to refine the position of the pole (Figure 5). The analysis shows two set of clustered solutions within 10° of radius that had Chi-Sq values within 10% of the lowest value, centered at ecliptic longitude-latitude (9°, 39°) and (177°, 28°).

The two best solutions (lower Chi-Sq and RMS) are reported in Table II. The sidereal period was obtained by averaging the two solutions found in the pole search process. Typical errors in the pole solution are ± 10° and the uncertainty in sidereal period has been evaluated as a rotational error of 20° over the total time span of the dense data set. Figure 6 shows the shape model (first solution with lower Chi-Sq and RMS) while Figure 7 shows the fit between the model (black line) and some observed lightcurves (red points).

λ °	β °	Sidereal Period (hours)	Chi-Sq	RMS
9	38	6.96397 ± 0.00002	0.51225	0.0175
178	28		0.53161	0.0178

Table II. The two spin axis solutions for 374 Burgundia (ecliptic coordinates) with an uncertainty of ± 10 degrees. The sidereal period was the average of the two solutions found in the pole search process.

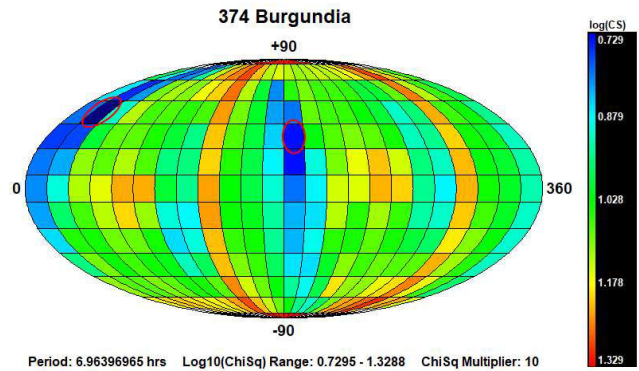


Figure 4: Pole search distribution. The dark blue region indicates the smallest Chi-Sq value while the dark red region indicates the largest.

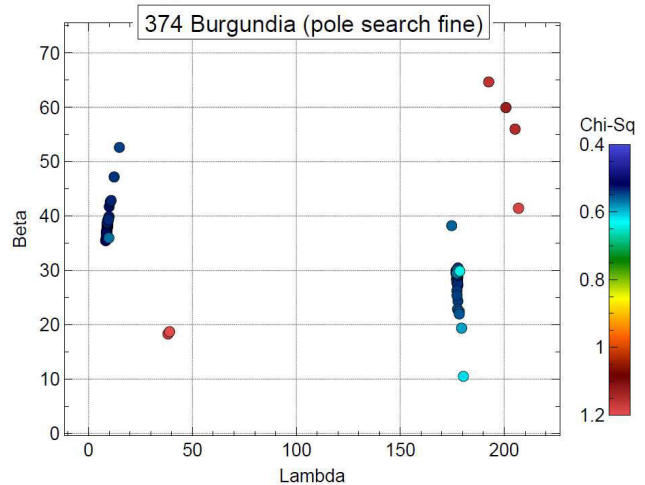


Figure 5: The “fine” pole search shows two clustered solutions centered at ecliptic longitude-latitude pairs (9°, 39°) and (177°, 28°) with radius approximately of 10° and Chi-Sq values within 10% of the lowest value.

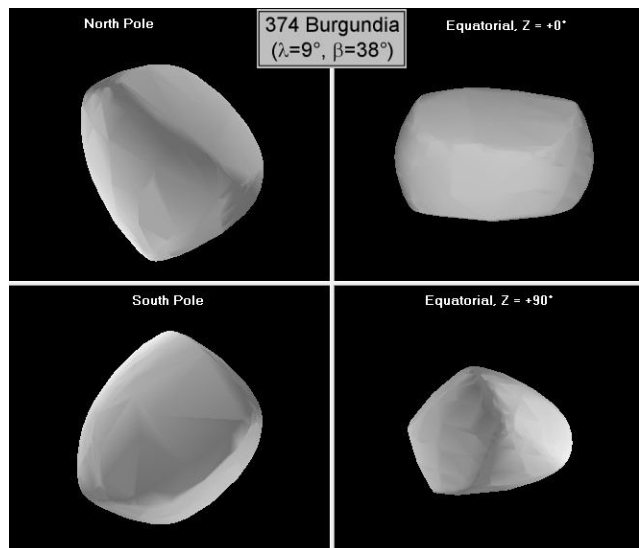


Figure 6: The shape model for 374 Burgundia ($\lambda = 9^\circ$, $\beta = 38^\circ$).

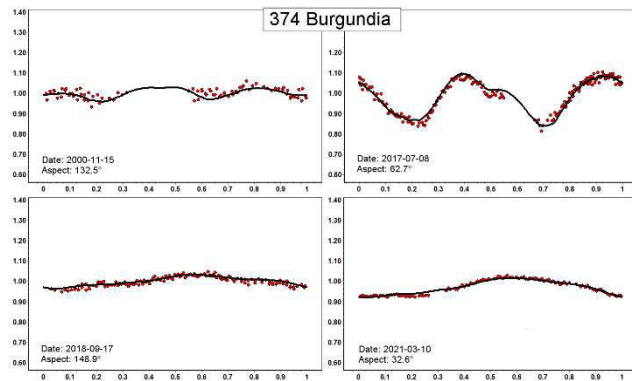


Figure 7: Model fit (black line) versus observed lightcurves (red points) for ($\lambda = 9^\circ$, $\beta = 38^\circ$) solution.

References

ALCDEF (2021). Asteroid Lightcurve Data Exchange Format web site. <http://www.alcdef.org/>

AstDyS-2 (2020). Asteroids - Dynamic Site. <https://newton.spacedys.com/astdys/>

BDW Publishing (2016). <http://www.minorplanetobserver.com/MPOSoftware/MPOLCInvert.htm>

Durech, J.; Kaasalainen, M.; Warner, B.D.; Fauerbach, M.; Marks, S.A.; Fauvaud, S.; Fauvaud, M.; Vugnon, J.-M.; Pilcher, F.; Bernasconi, L.; Behrend, R. (2009). "Asteroid models from combined sparse and dense photometric data." *A&A*, **493**, 291-297.

Durech, J.; Sidorin, V.; Kaasalainen, M. (2010). "DAMIT: a database of asteroid models." *A&A*, **513**, A46.

Franco, L.; Marchini, A.; Baj, G.; Scarfi, G.; Bacci, P.; Maestripieri, M.; Bacci, R.; Papini, R.; Salvaggio, F.; Banfi, M. (2019). "Lightcurves for 131 Vala, 374 Burgundia, 734 Brenda, and 929 Algunde." *Minor Planet Bulletin* **46**, 85-86.

Franco L.; Marchini, A.; Cavaglioni, L.; Papini, R.; Privitera, C.A.; Baj, G.; Galli, G.; Scarfi, G.; Aceti, P.; Banfi, M.; Bacci, P.; Maestripieri, M.; Mannucci, M.; Montigiani, N.; Tinelli, L.; Mortari, F. (2021). "Collaborative Asteroid Photometry from UAI: 2021 January-March." *Minor Planet Bulletin* **48**, 219-221.

UAI (2021). "Unione Astrofili Italiani" web site. <https://www.uai.it>

Warner, B.D.; Harris, A.W.; Pravec, P. (2009). "The asteroid lightcurve database." *Icarus* **202**, 134-146. Updated 2020 October. <http://www.minorplanet.info/lightcurvedatabase.html>

LIGHTCURVE PHOTOMETRY OPPORTUNITIES: 2021 JULY-SEPTEMBER

Brian D. Warner
Center for Solar System Studies / MoreData!
446 Sycamore Ave.
Eaton, CO 80615 USA
brian@MinorPlanetObserver.com

Alan W. Harris
MoreData!
La Cañada, CA 91011-3364 USA

Josef Durech
Astronomical Institute
Charles University
18000 Prague, CZECH REPUBLIC
durech@sirrah.troja.mff.cuni.cz

Lance A.M. Benner
Jet Propulsion Laboratory
Pasadena, CA 91109-8099 USA
lance.benner@jpl.nasa.gov

We present lists of asteroid photometry opportunities for objects reaching a favorable apparition and having no or poorly-defined lightcurve parameters. Additional data on these objects will help with shape and spin axis modeling using lightcurve inversion. We also include lists of objects that will be (or might be) radar targets. Lightcurves for these objects can help constrain pole solutions and/or remove rotation period ambiguities that might arise from using radar data alone.

We present several lists of asteroids that are prime targets for photometry during the period 2021 July-September.

In the first three sets of tables, "Dec" is the declination and "U" is the quality code of the lightcurve. See the latest asteroid lightcurve data base (LCDB from here on; Warner et al., 2009) documentation for an explanation of the U code:

<http://www.minorplanet.info/lightcurvedatabase.html>

The ephemeris generator on the CALL web site allows creating custom lists for objects reaching $V \leq 18.0$ during any month in the current year and up to five years in the future, e.g., limiting the results by magnitude and declination, family, and more.

http://www.minorplanet.info/PHP/call_OppLCDBQuery.php

We refer you to past articles, e.g., Warner et al. (2021) for more detailed discussions about the individual lists and points of advice regarding observations for objects in each list.

Once you've obtained and analyzed your data, it's important to publish your results. Papers appearing in the *Minor Planet Bulletin* are indexed in the Astrophysical Data System (ADS) and so can be referenced by others in subsequent papers. It's also important to make the data available at least on a personal website or upon request. We urge you to consider submitting your raw data to the ALCDEF database. This can be accessed for uploading and downloading data at

<http://www.alcdef.org>